Supplementary Information

Bioinspired Molecule Functionalized Cu with Strengthened CO Adsorption for Efficient CO Electroreduction to Acetate

Xuanzhao Lu,‡[a] Baozhen Yuan,‡[a] Yi Liu,[a] Li-Xia Liu*[b] and Jun-Jie Zhu*[a]

[a]*State Key Laboratory of Analytical Chemistry for Life Science, School of Chemistry and Chemical Engineering, Nanjing University, Nanjing 210023, China. E-mail: jjzhu@nju.edu.cn*
[b]*Jiangsu Key Laboratory of Green Synthetic Chemistry for Functional Materials, School of Chemistry and Materials Science, Jiangsu Normal University, Xuzhou 221116, China. E-mail: liulixia@jsnu.edu.cn*

‡These authors have contributed equally to this work.

1 Supporting figures and table

Figure S1

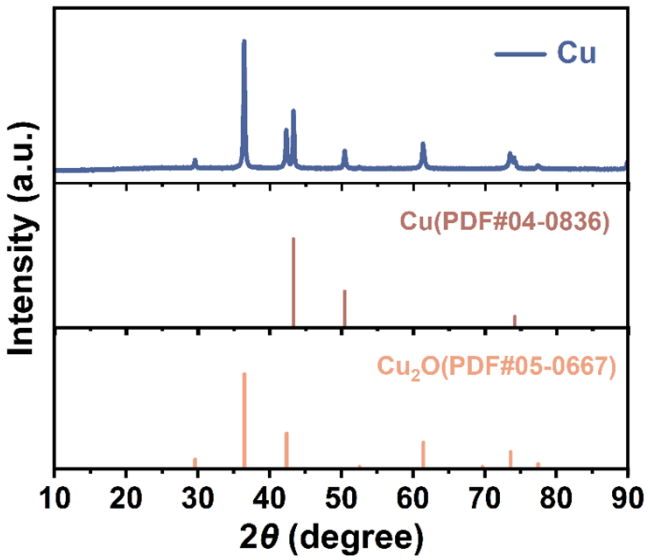

Figure S1. XRD pattern of Cu NPs.

Figure S2

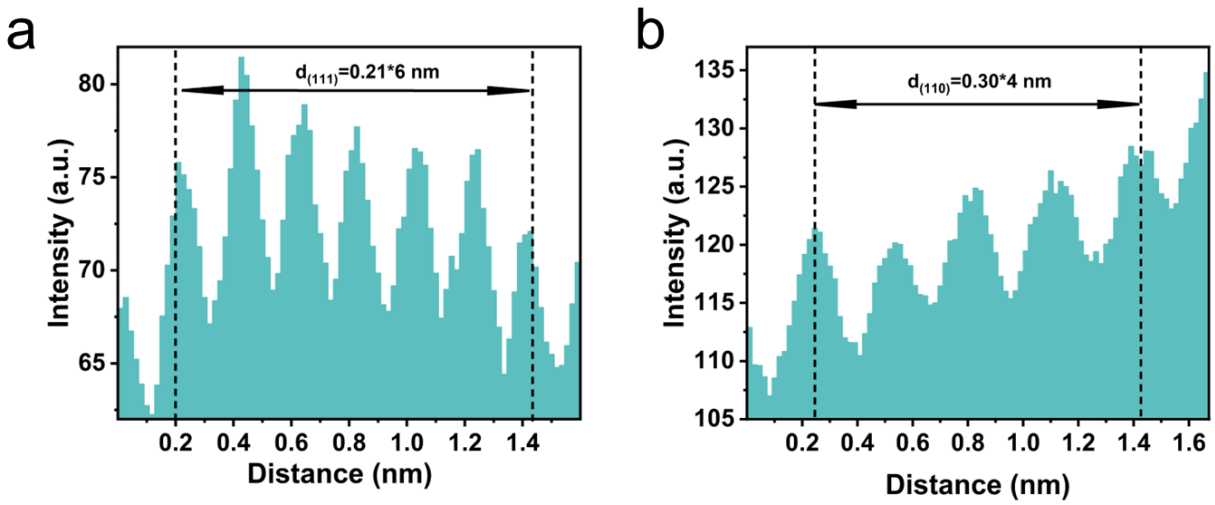

Figure S2. Line-scanning intensity profile from the area highlighted with the green rectangle in Figure 1b.

Figure S3

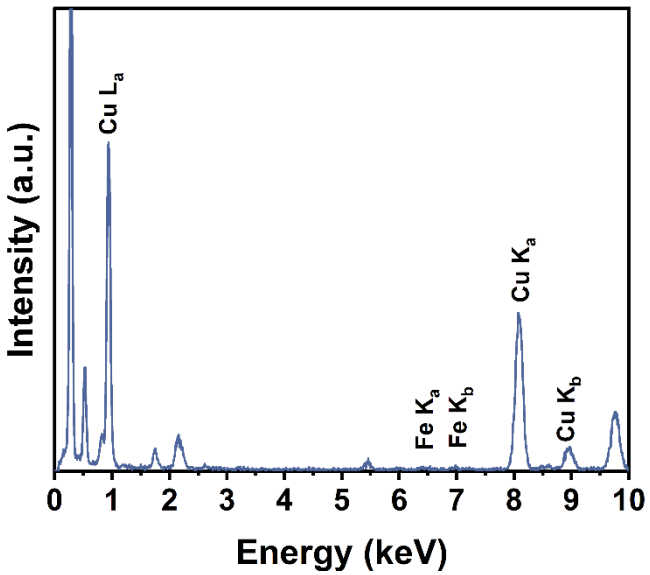

Figure S3. EDS spectrum of Cu NPs.

Figure S4

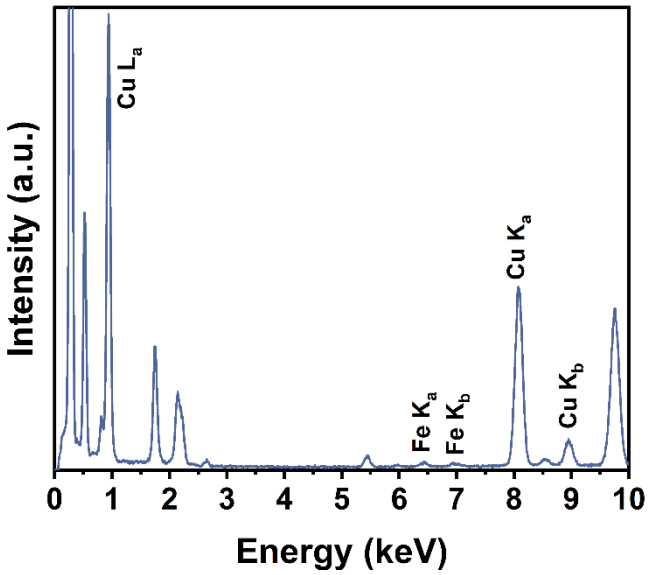

Figure S4. EDS spectrum of hemin/Cu-6.

Figure S5

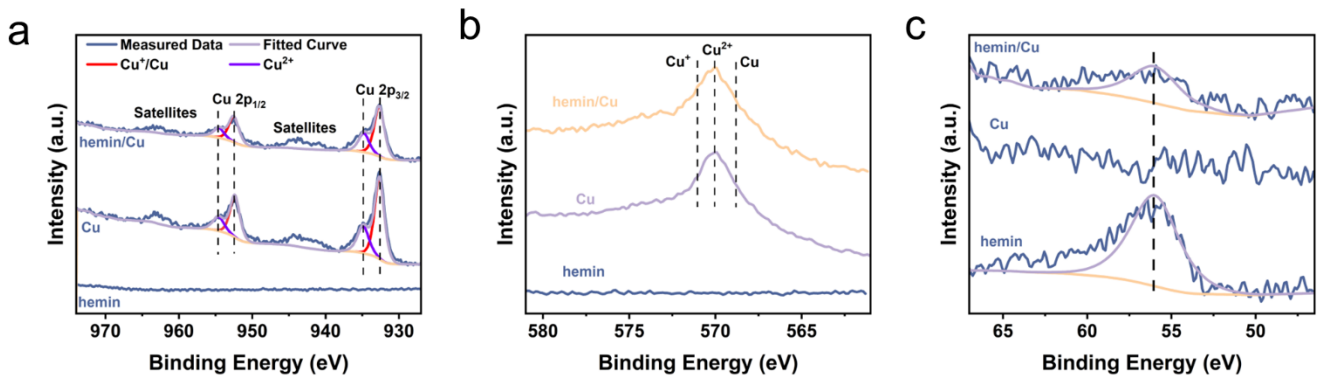

Figure S5. XPS spectra of the (a) Cu 2p, (b) Cu $L_3M_{4,5}M_{4,5}$ Auger, and (c) Fe 3p regions of hemin, Cu NPs, and hemin/Cu-6.

Figure S6

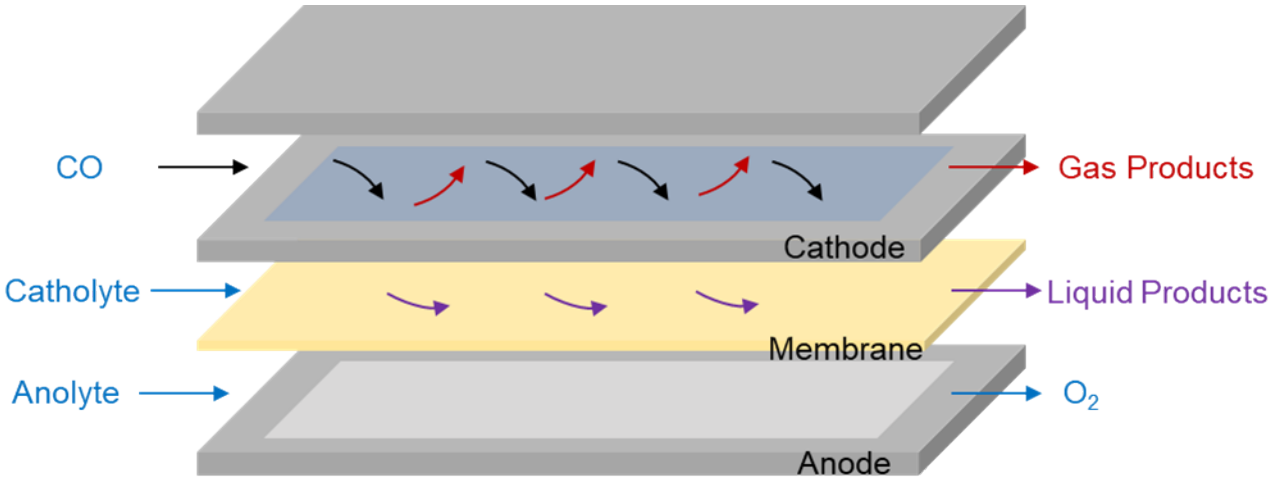

Figure S6. Schematic diagram of the flow cell.

Figure S7

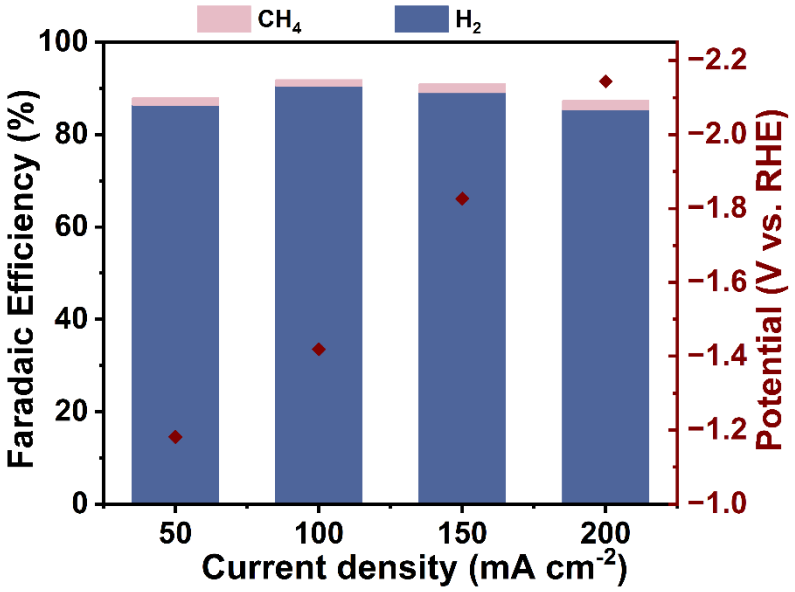

Figure S7. The FEs and potential measured for CO reduction on hemin.

Figure S8

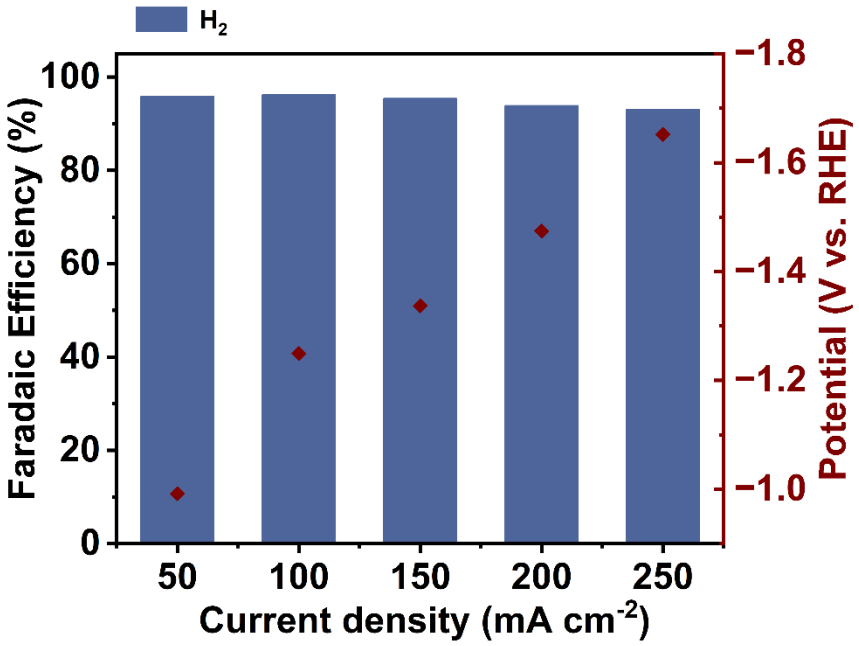

Figure S8. Electrocatalytic CO reduction product distributions of hemin/Cu-6 under Ar conditions.

Figure S9

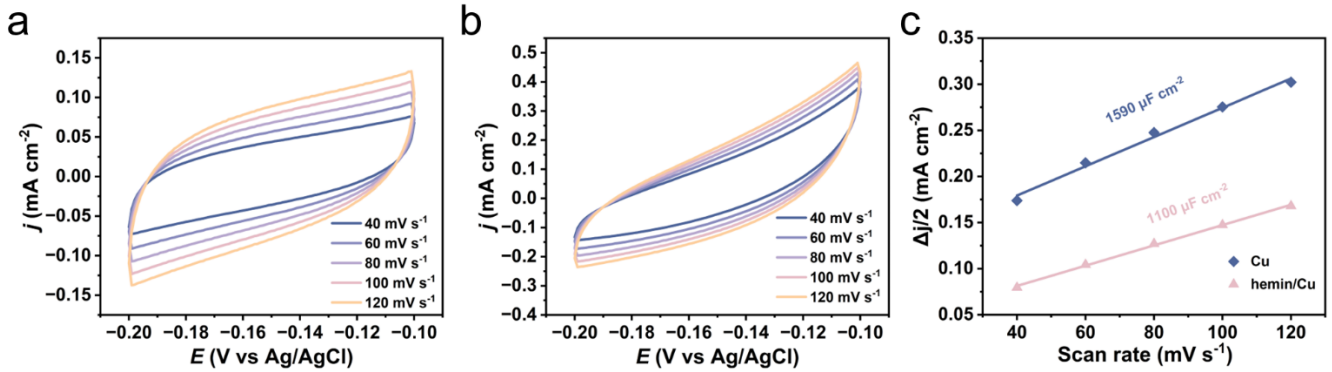

Figure S9. CV curves at different scan rates: (a) hemin/Cu-6 and (b) Cu NPs. (c) The capacitive current density differences at -0.15 V vs Ag/AgCl plotted against the scan rates. The ECSA is calculated using the following formula: $A_{ECSA} = C_{dl}$ / (29 μF cm^{-2} per cm^2_{ECSA}). The ECSA determined by the CV method for hemin/Cu: A_{ECSA} = (1100 μF cm^{-2}) / (29 μF cm^{-2}per cm^2_{ECSA}) = 37.9 cm^2_{ECSA}. The ECSA determined by the CV method for Cu NPs: A_{ECSA} = (1590 μF cm^{-2}) / (29 μF cm^{-2} per cm^2_{ECSA}) = 54.8 cm^2_{ECSA}.

Figure S10

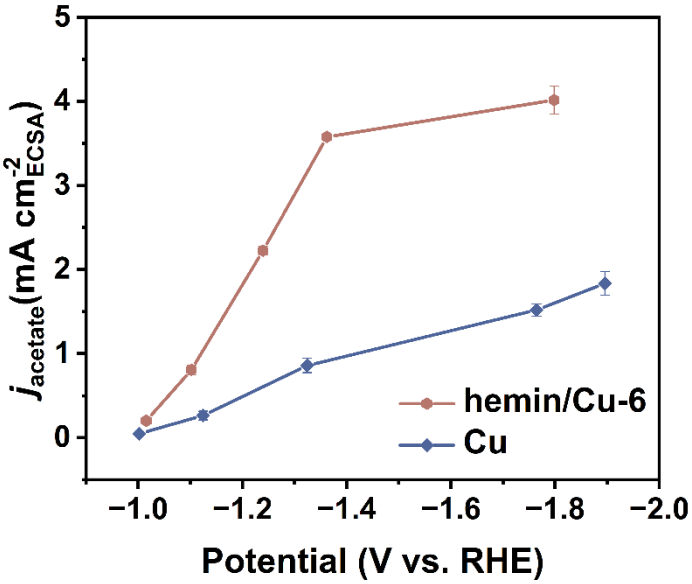

Figure S10. The normalized partial current densities towards acetate at different potentials of hemin/Cu-6 and Cu NPs.

Figure S11

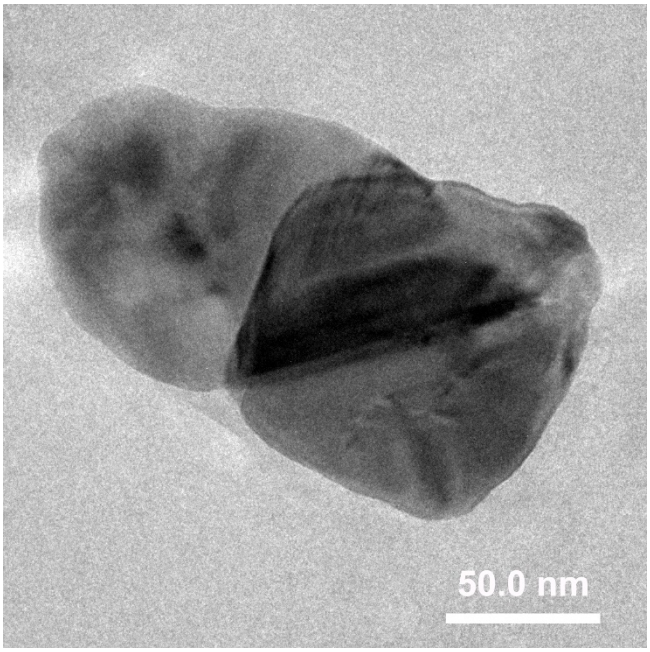

Figure S11. TEM image of hemin/Cu-6 after electrocatalysis test.

Figure S12

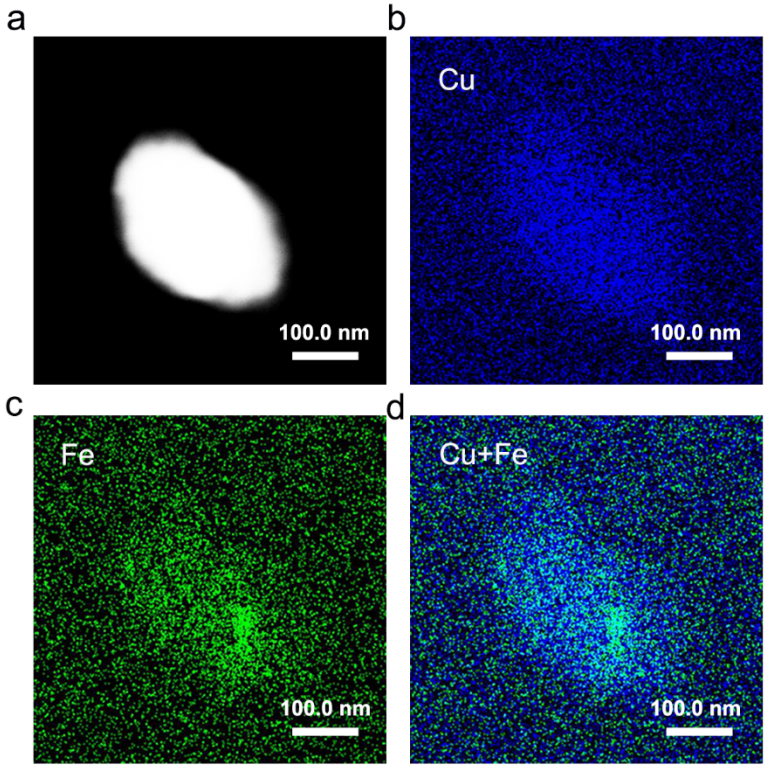

Figure S12. HAADF-STEM image and corresponding EDS mapping of hemin/Cu-6 catalysts after electrocatalysis test.

Figure S13

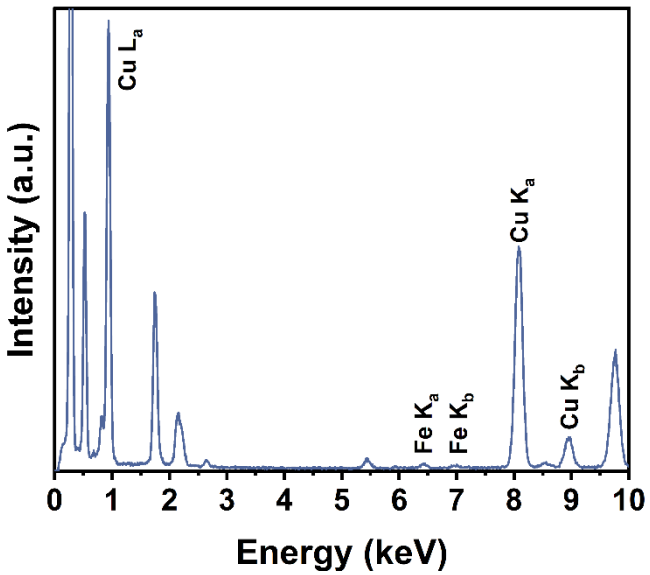

Figure S13. EDS spectrum of hemin/Cu-6 catalysts after electrocatalysis test.

Figure S14

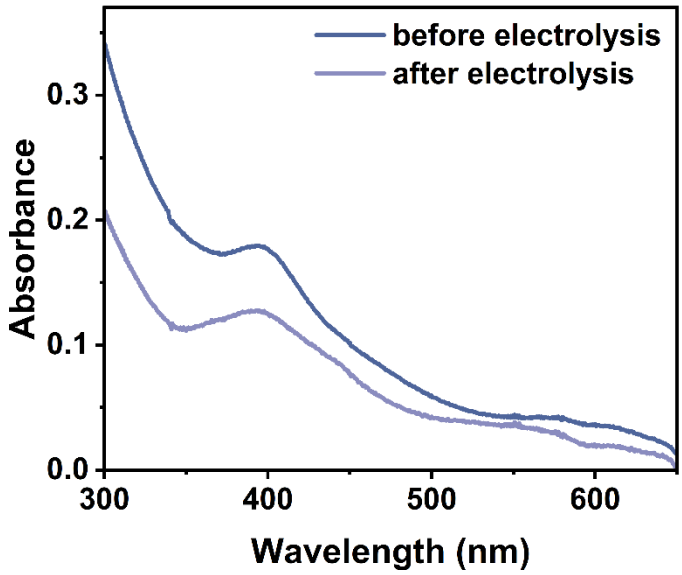

Figure S14. UV-vis spectroscopy of dissolved hemin from the fresh and used hemin/Cu-6 modified electrodes.

Figure S15

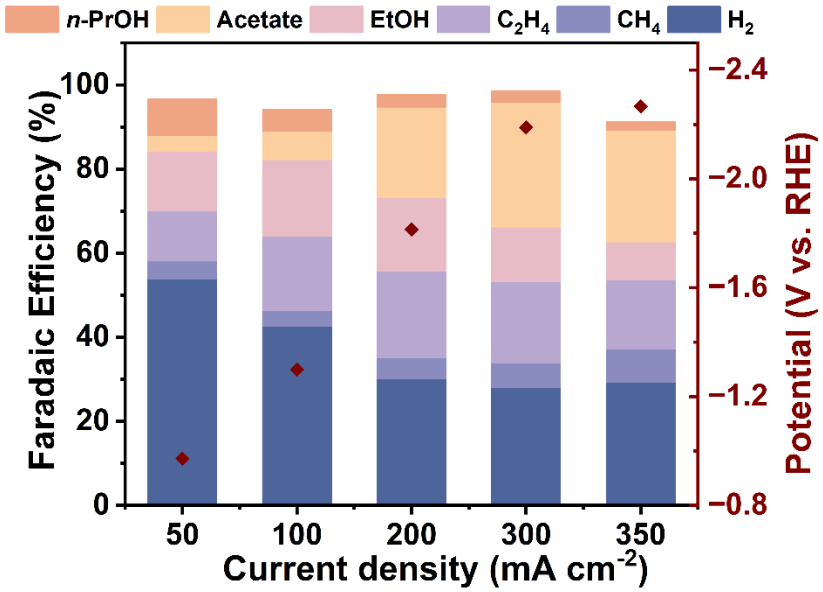

Figure S15. The product distribution at different current densities over protoporphyrin/Cu electrode.

Figure S16

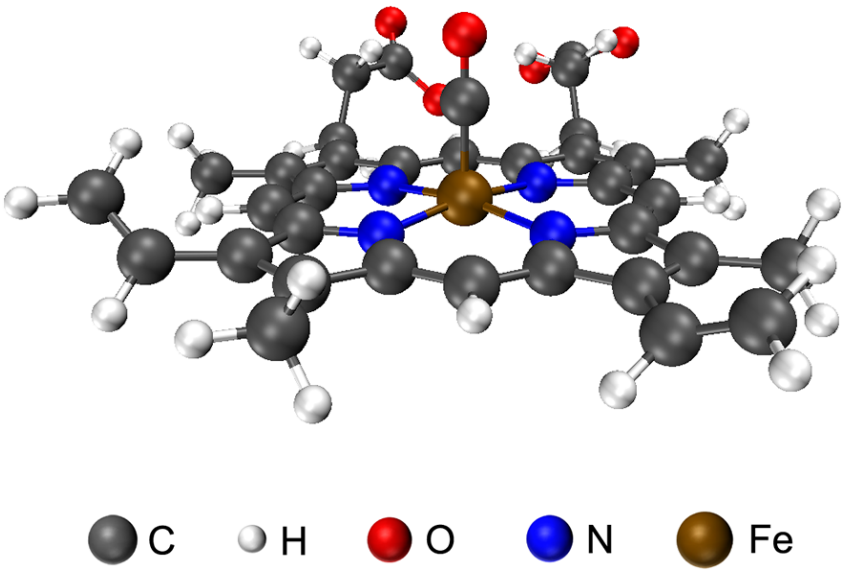

Figure S16. Optimized structures of heme-CO complex.

Figure S17

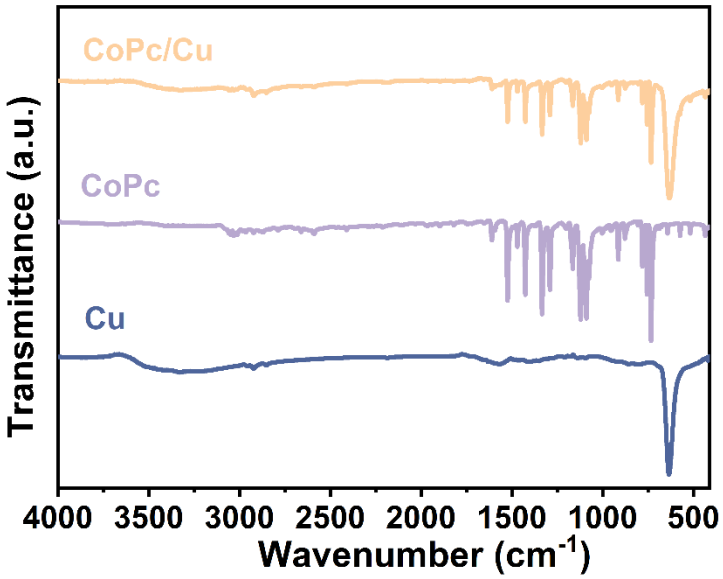

Figure S17. FTIR spectra of Cu, CoPc, and CoPc/Cu-6.

Figure S18

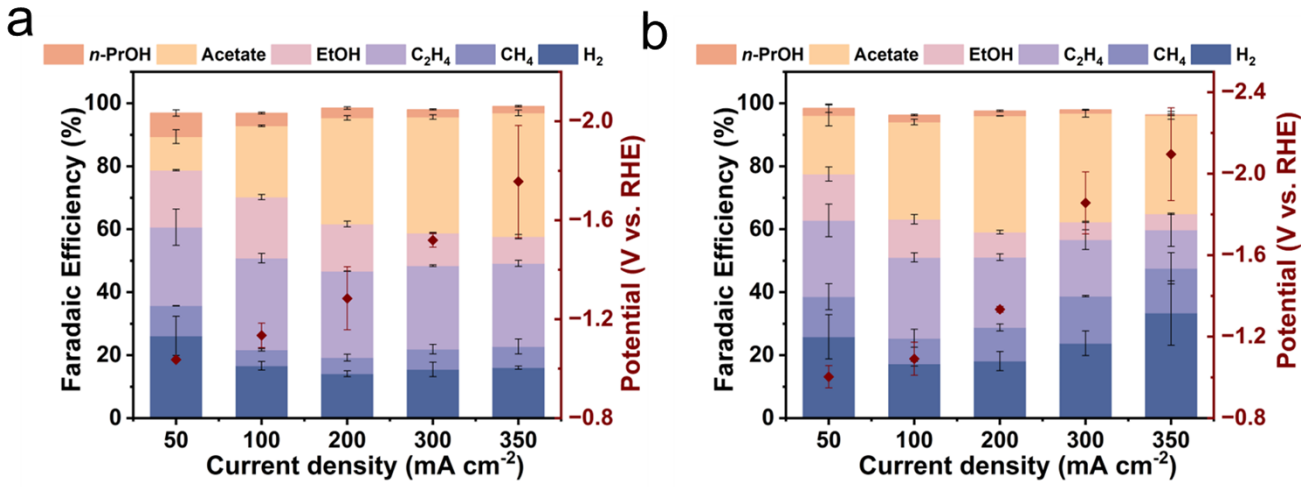

Figure S18. FEs and potentials measured for the electroreduction of CO on (a) CoPc/Cu-20, (b) CoPc/Cu-1.

Table S1

Comparison of electrochemical CO/CO_2-to-acetate performances with state-of-the-art Cu based catalysts.

Catalysts	CO/CO_2	Electrolyzers	Electrolyte	$FE_{acetate}$ (%)	$J_{acetate}$ (mA cm^{-2})	ref.
hemin/Cu-6	CO	Flow cell	1 M $KHCO_3$	45.2	~152.3	This work
Cu nanocube	CO	Flow cell	0.5 M $KHCO_3$	43	~200	1
$(Cu)_n$,$(Ag)_m$ clusters	CO_2	H cell	0.5 M $KHCO_3$	21.2	N/A	2
OD-Cu	CO	Flow cell	0.5 M KOH	18.9	45	3
			1 M KOH	29.6	105	
			2 M KOH	31.8	97.92	
Cu-Au	CO	Flow cell	1 M KOH	39	217	4
Cu nanosheets	CO	Flow cell	0.5 M KOH	25	25	5
			1 M KOH	33.1	33.1	
			2 M KOH	48	131	
ERD-Cu	CO_2	Flow cell	0.1 M $KHCO_3$	6.7	N/A	6
Cu Foil	CO_2	Flow cell	0.1 M $KHCO_3$	0.3	7	7
Mesostructured Cu	CO_2	Flow cell	0.1 M $KHCO_3$	2.54	0.66	8
OD-Cu	CO	H cell	1 M KOH	61	N/A	9
			0.1 M KOH	~18		
$Cu_{45.2}$/GDY	CO	Flow cell	1 M KOH	~20	~42	10
Cu-N-C single site catalyst	CO	Flow cell	1 M KOH	30	48	11
Cu	CO	Flow cell	1 M KOH	16.3	81.5	12
CuTCPP@$Cu(OH)_2$	CO_2	H cell	0.5 M $EMIMBF_4$	26.1	N/A	13

[a] N/A=Not available from this source.

2 Supporting references

1. P. Zhu, C. Xia, C.-Y. Liu, K. Jiang, G. Gao, X. Zhang, Y. Xia, Y. Lei, H. N. Alshareef, T. P. Senftle and H. Wang, *Proc. Natl. Acad. Sci. U. S. A.*, 2021, **118**, e2010868118.
2. Y. Wang, D. Wang, C. J. Dares, S. L. Marquard, M. V. Sheridan and T. J. Meyer, *Proc. Natl. Acad. Sci. U. S. A.*, 2018, **115**, 278-283.
3. M. Jouny, W. Luc and F. Jiao, *Nat. Catal.*, 2018, **1**, 748-755.
4. Q. Sun, Y. Zhao, X. Tan, C. Jia, Z. Su, Q. Meyer, M. I. Ahmed and C. Zhao, *ACS Catal.*, 2023, **13**, 5689-5696.
5. W. Luc, X. Fu, J. Shi, J.-J. Lv, M. Jouny, B. H. Ko, Y. Xu, Q. Tu, X. Hu, J. Wu, Q. Yue, Y. Liu, F. Jiao and Y. Kang, *Nat. Catal.*, 2019, **2**, 423-430.
6. P. De Luna, R. Quintero-Bermudez, C.-T. Dinh, M. B. Ross, O. S. Bushuyev, P. Todorović, T. Regier, S. O. Kelley, P. Yang and E. H. Sargent, *Nat. Catal.*, 2018, **1**, 103-110.
7. K. P. Kuhl, E. R. Cave, D. N. Abram and T. F. Jaramillo, *Energy Environ. Sci.*, 2012, **5**, 7050-7059.
8. T. Kim, A. Kargar, Y. Luo, R. Mohammed, E. Martinez-Loran, A. Ganapathi, P. Shah and D. P. Fenning, *ACS Appl. Energy Mater.*, 2018, **1**, 1965-1972.
9. C. W. Li, J. Ciston and M. W. Kanan, *Nature*, 2014, **508**, 504-507.
10. W. Rong, H. Zou, W. Zang, S. Xi, S. Wei, B. Long, J. Hu, Y. Ji and L. Duan, *Angew. Chem. Int. Ed.*, 2021, **60**, 466-472.
11. X. Fu, Y. Wang, H. Shen, Y. Yu, F. Xu, G. Zhou, W. Xie, R. Qin, C. Dun, C. W. Pao, J. L. Chen, Y. Liu, J. Guo, Q. Yue, J. J. Urban, C. Wang and Y. Kang, *Mater. Today Phys.*, 2021, **19**, 100418.
12. M. Jouny, J.-J. Lv, T. Cheng, B. H. Ko, J.-J. Zhu, W. A. Goddard and F. Jiao, *Nat. Chem.*, 2019, **11**, 846-851.
13. Y.-H. Xiao, Y.-X. Zhang, R. Zhai, Z.-G. Gu and J. Zhang, *Sci. China Mater.*, 2022, **65**, 1269-1275.